



**Using Engineered Scaffold Interactions to Reshape
MAP Kinase Pathway Signaling Dynamics**

Caleb J. Bashor, *et al.*
Science **319**, 1539 (2008);
DOI: 10.1126/science.1151153

**The following resources related to this article are available online at
www.sciencemag.org (this information is current as of March 18, 2008):**

Updated information and services, including high-resolution figures, can be found in the online version of this article at:

<http://www.sciencemag.org/cgi/content/full/319/5869/1539>

Supporting Online Material can be found at:

<http://www.sciencemag.org/cgi/content/full/319/5869/1539/DC1>

A list of selected additional articles on the Science Web sites **related to this article** can be found at:

<http://www.sciencemag.org/cgi/content/full/319/5869/1539#related-content>

This article **cites 34 articles**, 9 of which can be accessed for free:

<http://www.sciencemag.org/cgi/content/full/319/5869/1539#otherarticles>

This article appears in the following **subject collections**:

Cell Biology

http://www.sciencemag.org/cgi/collection/cell_biol

Information about obtaining **reprints** of this article or about obtaining **permission to reproduce this article** in whole or in part can be found at:

<http://www.sciencemag.org/about/permissions.dtl>

tide systems (27). Along these lines, activation of the SP-NK1R system may not be a consistent feature of depressive illness. If, however, a pathological activation of the SP-NK1R system follows a history of alcohol dependence, similar to CRH, NK1 antagonism may have a considerable potential as a treatment for alcoholism.

References and Notes

- M. Ezzati, A. D. Lopez, A. Rodgers, S. van den Horn, C. J. Murray, *Lancet* **360**, 1347 (2002).
- K. D. Brownell, G. A. Marlatt, E. Lichtenstein, G. T. Wilson, *Am. Psychol.* **41**, 765 (1986).
- A. D. Lê et al., *Psychopharmacology (Berlin)* **135**, 169 (1998).
- M. Heilig, M. Egli, *Pharmacol. Ther.* **111**, 855 (2006).
- X. Liu, F. Weiss, *J. Neurosci.* **22**, 7856 (2002).
- R. Sinha, C. S. Li, *Drug Alcohol Rev.* **26**, 25 (2007).
- M. Heilig, G. F. Koob, *Trends Neurosci.* **30**, 399 (2007).
- A. Holmes, M. Heilig, N. M. J. Rupniak, T. Steckler, G. Griebel, *Trends Pharmacol. Sci.* **24**, 580 (2003).
- T. L. Ripley, C. A. Gadd, C. De Felipe, S. P. Hunt, D. N. Stephens, *Neuropharmacology* **43**, 1258 (2002).
- P. Murtra, A. M. Sheasby, S. P. Hunt, F. C. De, *Nature* **405**, 180 (2000).
- T. Furmark et al., *Biol. Psychiatry* **58**, 132 (2005).
- Materials and methods are available as supporting material on Science Online.
- C. De Felipe et al., *Nature* **392**, 394 (1998).
- J. C. Crabbe, T. J. Phillips, *Psychopharmacology (Berlin)* **174**, 539 (2004).
- M. A. Schuckit, T. L. Smith, J. Kalmijn, *Alcohol. Clin. Exp. Res.* **28**, 1449 (2004).
- A. K. Amegadzie et al., "Preparation of triazole derivatives as tachykinin receptor antagonists." (WO 2003091226 A1, World Intellectual Property Organization); published online 6 November 2003, www.wipo.int/pctdb/en/wo.jsp?wo=2003091226.
- C. D. Spielberger, R. L. Gorsuch, R. E. Lushene, *Manual for the State-Trait Anxiety Inventory* (Consulting Psychologist Press, Palo Alto, CA, 1970).
- P. J. Lang, M. M. Bradley, B. N. Cuthbert, *International Affective Picture System (IAPS): Technical Manual and Affective Ratings* (The Center for Research in Psychophysiology, Univ. of Florida, Gainesville, FL, 1995).
- J. M. Gilman, D. Hommer, *Addiction Biol.*, in press.
- A. L. Brody et al., *Arch. Gen. Psychiatry* **59**, 1162 (2002).
- N. H. Naqvi, D. Rudrauf, H. Damasio, A. Bechara, *Science* **315**, 531 (2007).
- A. Heinz et al., *Alcohol. Clin. Exp. Res.* **31**, 1138 (2007).
- B. A. Flannery, S. A. Poole, R. J. Gallop, J. R. Volpicelli, *J. Stud. Alcohol* **64**, 120 (2003).
- S. S. O'Malley, S. Krishnan-Sarin, C. Farren, R. Sinha, M. J. Kreek, *Psychopharmacology (Berlin)* **160**, 19 (2002).
- S. T. Tiffany, *Psychol. Rev.* **97**, 147 (1990).
- M. S. Kramer et al., *Science* **281**, 1640 (1998).
- J. M. Lundberg, T. Hökfelt, *Trends Neurosci.* **6**, 325 (1983).
- We thank nurse manager J. Johnson and her treatment staff at the 15E Unit of the NIH Clinical Center, as well as D. Hill, L. Doty, and C. Jones for their invaluable contributions to this study. R. Anton, S. Thomas, R. Miranda, and P. Monti are gratefully acknowledged for input in the design stages of the clinical study. Supported by the intramural research budget of the National Institute on Alcohol Abuse and Alcoholism, NIH. This work was carried out under a Collaborative Research and Development Agreement (CRADA) between the U.S. Government and Eli Lilly and Co. All coauthors so indicated are employees of Eli Lilly and Co.; the remaining authors have no conflict of interest to disclose.

Supporting Online Material

www.sciencemag.org/cgi/content/full/1153813/DC1

Materials and Methods

Fig. S1

Tables S1 to S3

References

5 December 2007; accepted 6 February 2008

Published online 14 February 2008;

10.1126/science.1153813

Include this information when citing this paper.

Using Engineered Scaffold Interactions to Reshape MAP Kinase Pathway Signaling Dynamics

Caleb J. Bashor,^{1,2} Noah C. Helman,¹ Shude Yan,¹ Wendell A. Lim^{1*}

Scaffold proteins link signaling molecules into linear pathways by physically assembling them into complexes. Scaffolds may also have a higher-order role as signal-processing hubs, serving as the target of feedback loops that optimize signaling amplitude and timing. We demonstrate that the Ste5 scaffold protein can be used as a platform to systematically reshape output of the yeast mating MAP kinase pathway. We constructed synthetic positive- and negative-feedback loops by dynamically regulating recruitment of pathway modulators to an artificial binding site on Ste5. These engineered circuits yielded diverse behaviors: ultrasensitive dose response, accelerated or delayed response times, and tunable adaptation. Protein scaffolds provide a flexible platform for reprogramming cellular responses and could be exploited to engineer cells with novel therapeutic and biotechnological functions.

In cells, signaling proteins that make up a pathway are often physically organized into complexes by scaffold proteins (1–3). Scaffolds direct information flow; they promote signaling between proper protein partners and prevent improper cross talk. Scaffolds may also play a role in shaping the quantitative response behavior of a pathway. The scaffold complex could serve as a central hub for feedback loops that modulate the recruitment or activity of

pathway members on the scaffold. Such feedback loops could tune pathway dose response and dynamics—the change in output over time. Quantitative response behavior is critical for signaling; the behavior of a pathway must match its specific physiological function (4). Scaffolds may therefore provide a platform for evolutionarily tuning response behaviors for optimal fitness (5, 6).

We used a synthetic biology approach to explore this hypothesis; we tested whether a scaffold protein can be used as a platform for engineering synthetic feedback loops and whether these loops can be used to systematically reshape pathway response behavior (7). We used the yeast mating mitogen-activated protein (MAP) kinase pathway as a model system, because it is highly tractable for pathway engineer-

ing. First, proper connectivity of this pathway is dependent on the scaffold protein Ste5, which binds the three core kinases—Ste11 (a MAP kinase kinase or MAPKKK), Ste7 (a MAP kinase kinase, or MAPKK), and Fus3 (a MAP kinase, or MAPK)—that successively phosphorylate and activate one another (Fig. 1A) (8, 9). The critical role in determining pathway connectivity is highlighted by the observation that chimeric scaffolds can be used to redirect pathway input and output linkages (10, 11). Second, MAP kinase pathways appear to be functionally plastic; they are found in all eukaryotic species, but in individual cases display widely varied behaviors. For example, the yeast mating pathway shows a largely linear transcriptional response (12–14), whereas the *Xenopus* oocyte maturation pathway displays a switchlike dose response (15). MAPK pathways also show diverse dynamic behavior; some yield a sustained response to stimulation, whereas others show a pulselike transient response. These distinct pathway dynamics are critical for determining physiological output (16–21).

Our goal was to overlay the endogenous mating pathway with synthetic feedback loops in order to systematically alter its response to mating pheromone (α -factor) stimulation. A simple way to construct a synthetic feedback loop would be to dynamically recruit pathway modulators to the scaffold in a manner that is dependent on pathway output. We first tested whether constitutive recruitment of modulator proteins could alter pathway flux. We created a new recruitment site on Ste5 by fusing a leucine zipper heterodimerization module (22) to its C terminus. Modulator proteins fused to complementary zippers were expressed and recruited to the scaffold (Fig. 1B). Two pathway modulators were recruited:

¹Department of Cellular and Molecular Pharmacology, University of California at San Francisco, 600 16th Street, San Francisco, CA 94158, USA. ²Graduate Group in Biophysics, University of California at San Francisco, 600 16th Street, San Francisco, CA 94158, USA.

*To whom correspondence should be addressed. E-mail: lim@cmp.ucsf.edu

Ste50 and Msg5 (Fig. 1A). Ste50 is a positive modulator, an adaptor that promotes interaction of the MAPKKK Ste11 with its upstream activator, the p21-activated protein kinase (PAK)-like kinase, Ste20 (23, 24). Msg5 is a negative modulator, a MAPK phosphatase that inactivates phosphorylated Fus3 MAPK (25, 26). When artificially recruited to the Ste5 scaffold through a

leucine zipper interaction, Msg5 and Ste50 showed strong but opposite effects on pathway output, measured using a fluorescent transcriptional reporter [see supporting online text and (27)]. Recruitment of the positive modulator (Ste50) increased the steady-state output of the activated pathway, whereas recruitment of the negative modulator (Msg5) decreased output,

nearly eliminating any input-stimulated response. Unrecruited Ste50 and Msg5 had much smaller effects when expressed at the same level. Thus, the impact of modulators on pathway flux was enhanced by recruitment to the scaffold.

To build synthetic feedback loops, we then placed the modulators under the control of a mating-dependent promoter (*pFIG1*) (Fig. 2A),

Fig. 1. Tuning output from yeast mating MAPK pathway by artificially recruiting positive or negative modulators to Ste5 scaffold protein.

(A) Yeast mating pathway: α -factor activates receptor, Ste2, and G_β subunit, Ste4; activated Ste4 recruits Ste5 complex to membrane, allowing PAK-like kinase Ste20 (membrane-localized) to activate MAPKKK Ste11; Ste11 and downstream kinases, Ste7 (MAPKK) and Fus3 (MAPK), are colocalized on the scaffold; activation of cascade leads to transcriptional program [reporter: Fus1 promoter-GFP (green fluorescent protein)]. We have used pathway modulators outside of core cascade: Ste50 (positive, blue) promotes activation of Ste11 by Ste20; Msg5 (negative, red) is MAPK phosphatase that deactivates Fus3. (B) Synthetic recruitment of pathway modulators to Ste5 scaffold via leucine zipper interaction. A basic zipper was fused to Ste5, and the complementary acidic zipper was fused to modulators (zipper $K_d = 6.1$ nM; see supporting online text). Control (“unrecruited”) modulators were fused to noncomplementary zipper. Pathway output was assessed via *pFUS1*-GFP expression. Basal output is before

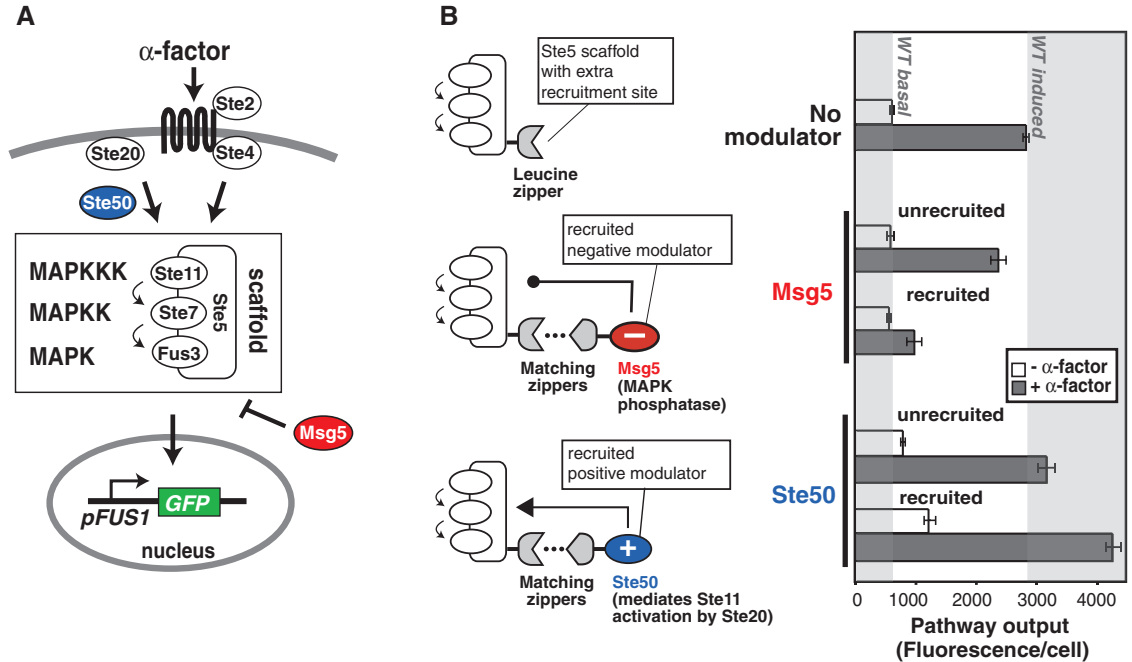
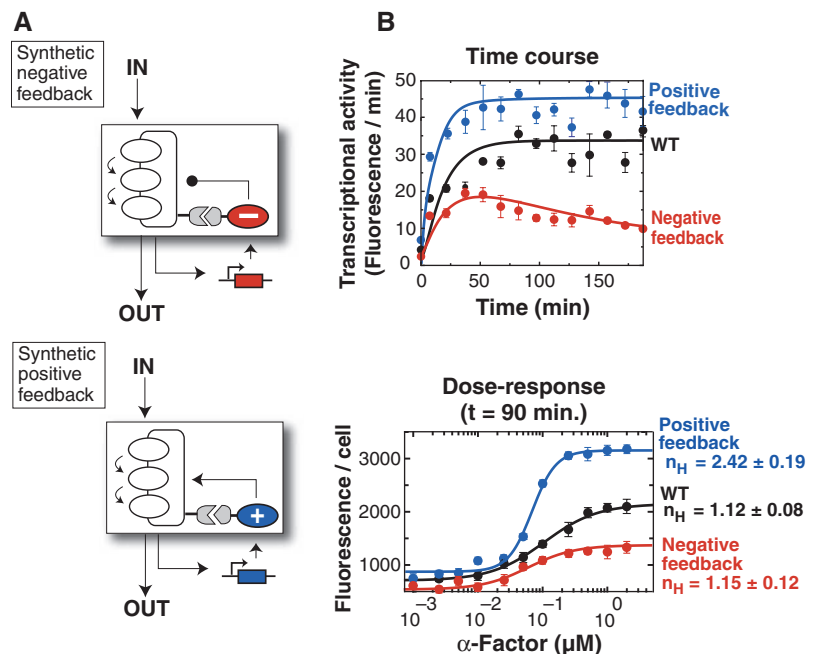


Fig. 2. Building synthetic feedback loops by dynamically regulating recruitment of modulators to the Ste5 scaffold. (A) Negative- and positive-feedback loop design. Modulator-zipper fusions (negative, Msg5; positive, Ste50) are expressed from a mating-responsive promoter (*pFIG1*). Stimulation induces expression of the modulator, which is then recruited to the Ste5-complex (boxed), where it can modulate pathway flux. (B) Behavior of synthetic feedback loops. All circuits were in *far1 Δ* strain (designated “WT”), which does not undergo mating-induced cell cycle arrest. Thus, cells are uniform in size, facilitating fluorescence-activated cell sorting analysis. Negative-feedback circuit (red) shows an initial rate of activation similar to the wild-type, but peaks at ~ 35 min, and adapts to steady-state output about one-third that of wild-type. Positive-feedback circuit (blue) shows dynamics similar to wild type’s, but with steady-state output ~ 1.5 times as great as wild type’s. The dose-response curves (bottom) show that the positive-feedback circuit displays more switchlike activation (apparent Hill coefficient $n_H = 2.42 \pm 0.19$ versus wild-type, $n_H = 1.12 \pm 0.08$). Points represent mean values for three experiments \pm standard deviation. Pathway is activated with $2 \mu\text{M}$ α -factor. Best-fit lines generated as described in supporting online text.



stimulation; induced output is 120 min after stimulation with $2 \mu\text{M}$ α -factor (saturating). Error bars represent standard deviation of three experiments. Strains were *ste5 Δ* with integrated Ste5-zipper fusion expressed from *pSTE5* promoter. Modulator-zipper fusions were integrated and expressed from *pCYC1* promoter. Reversed orientation of zippers (fig. S2E) gave similar results.

so that they were only expressed upon pathway activation. The positive-feedback circuit (using Ste50) increased steady-state pathway output and led to a more switchlike dose response (apparent Hill coefficient n_H increased from 1.12 to 2.42). Similar behavior was generated using positive-feedback loops in which constitutive pathway alleles were expressed from a mating-responsive promoter (28).

The engineered negative-feedback circuit (using Msg5) displays adaptation. The cells initially responded like wild-type, but after 35 min, showed a decrease in output, even with continued stimulation. Adaptation is critical for homeostatic and sensing systems. It can be important to limit the magnitude and duration of an output that is harmful or has a high metabolic cost. Adaptation is also used in sensing systems (e.g., vision or chemotaxis) that automatically desensitize to a continuous stimulus, allowing for detection of input changes over a large dynamic range (29, 30).

One advantage of engineered feedback loops is the ability to systematically explore how the alteration of specific circuit parameters affects pathway behavior. Simulations indicate that adaptation in the simple negative-feedback circuit can be tuned by adjusting feedback strength (Fig. 3A). We explored two methods for adjusting feedback strength. First, we changed the strength of the leucine zipper interaction used to recruit Msg5 (Fig. 3B), using a set of three leucine zipper pairs that bind with the following affinities: $K_d = 6, 40,$ and 810 nM (22). Second, we changed the strength of the promoter con-

trolling expression of recruited Msg5 (Fig. 3C), using a pair of mating promoters: *pFIG1* (strong) and *pPRM2* (weak) (see fig. S4). As predicted, either method results in a decrease in the steady-state pathway output.

Because these synthetic feedback circuits rely on modulator recruitment, they could be regulated by competitive interactions that block recruitment. We tested whether competitors could be used to build more complex negative-feedback circuits that displayed a pulslike activation response (high maximal output followed by low steady-state output) (Fig. 4A). We constitutively expressed a decoy leucine zipper that competes with the scaffold protein (Ste5-zipper) for binding to the negative modulator (Msg5-zipper). Because the decoy has a higher affinity, it initially acts as a sink; after pathway activation, newly expressed negative modulator bound to the decoy zipper, preventing recruitment to the scaffold. Only after the decoy zipper is saturated is additionally expressed negative modulator recruited to the scaffold, which results in pathway repression. Indeed, this delayed negative-feedback loop led to a pulslike response (higher maximal output, followed by decrease in output). Moreover, the sharpness of the response could be modulated by adjusting the level at which the decoy zipper was expressed; higher decoy expression led to a more pulslike response.

The interplay of competing scaffold interactions and variable expression can be used to generate additional dynamic behaviors, including systems with faster or slower response time. The

rise time of a pathway—how fast a response occurs after input—can be critical for function. A pathway that detects a toxic stress may require a fast response. A delayed response may be required if the response is energetically very costly or if there is a high level of input noise (a delay circuit could prevent misactivation by transient input fluctuations, while still allowing activation by a sustained input).

We were able to alter the mating pathway to show accelerated response time, while maintaining a wild-type level of maximal pathway output (Fig. 4B). In this accelerator circuit, the positive modulator (Ste50-zipper) was constitutively expressed, but the negative modulator (Msg5-zipper, high affinity) was inducibly expressed. This result supports the idea that negative feedback can speed the time it takes to reach steady-state (31), albeit at a reduced steady-state output. But here, the wild-type magnitude of output is achieved by the added presence of the positive modulator.

We also generated a delay circuit by constitutively expressing a negative modulator (Msg5-zipper) and inducibly expressing a high-affinity decoy zipper (Fig. 4C). The pathway initially showed a weak response to stimulation because the recruited negative modulator kept the pathway off. After a delay of ~ 50 min, however, a small but sufficient level of pathway activation was reached, and expression of the high-affinity decoy zipper displaced the negative modulator, which allowed pathway activation.

Competition between positive and negative modulators can also be used to alter dose-response

Fig. 3. Strength of synthetic negative-feedback circuit can be tuned by either altering recruitment affinity or inducible expression level of negative modulator. (A) Computational model (see supporting online text) predicts that adjustments in negative-feedback gain should tune adaptation behavior. (B) Adjusting feedback gain by varying modulator recruitment strength. Three affinity variants of the leucine zipper (strong, $K_d = 6.1$ nM; medium, $K_d = 41$ nM; and weak, $K_d = 810$ nM) were fused to Msg5 (negative modulator). Promoter controlling modulator expression was constant (*pPRM2*). (C) Adjusting feedback gain by varying modulator promoter strength. Msg5-zipper is expressed from two mating-induced promoters: strong, *pFIG1*, and weak, *pPRM2* (fig. S4). Zipper fused to Msg5 was constant (weak). Orange plots in (B) and (C) show same strain (circuit with weak zipper and weak promoter). Points represent mean values for three experiments \pm standard deviation.

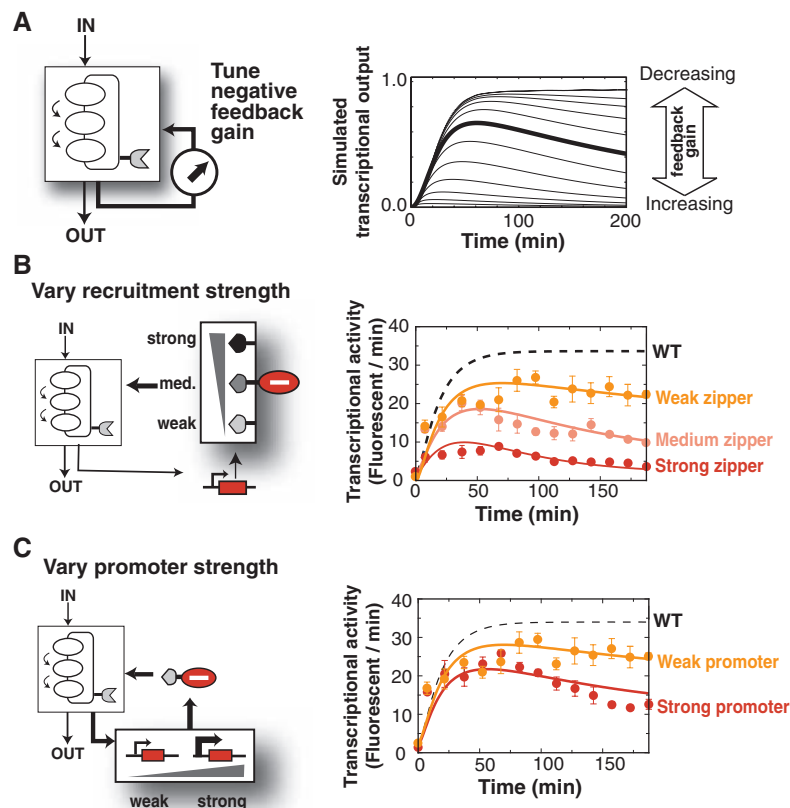
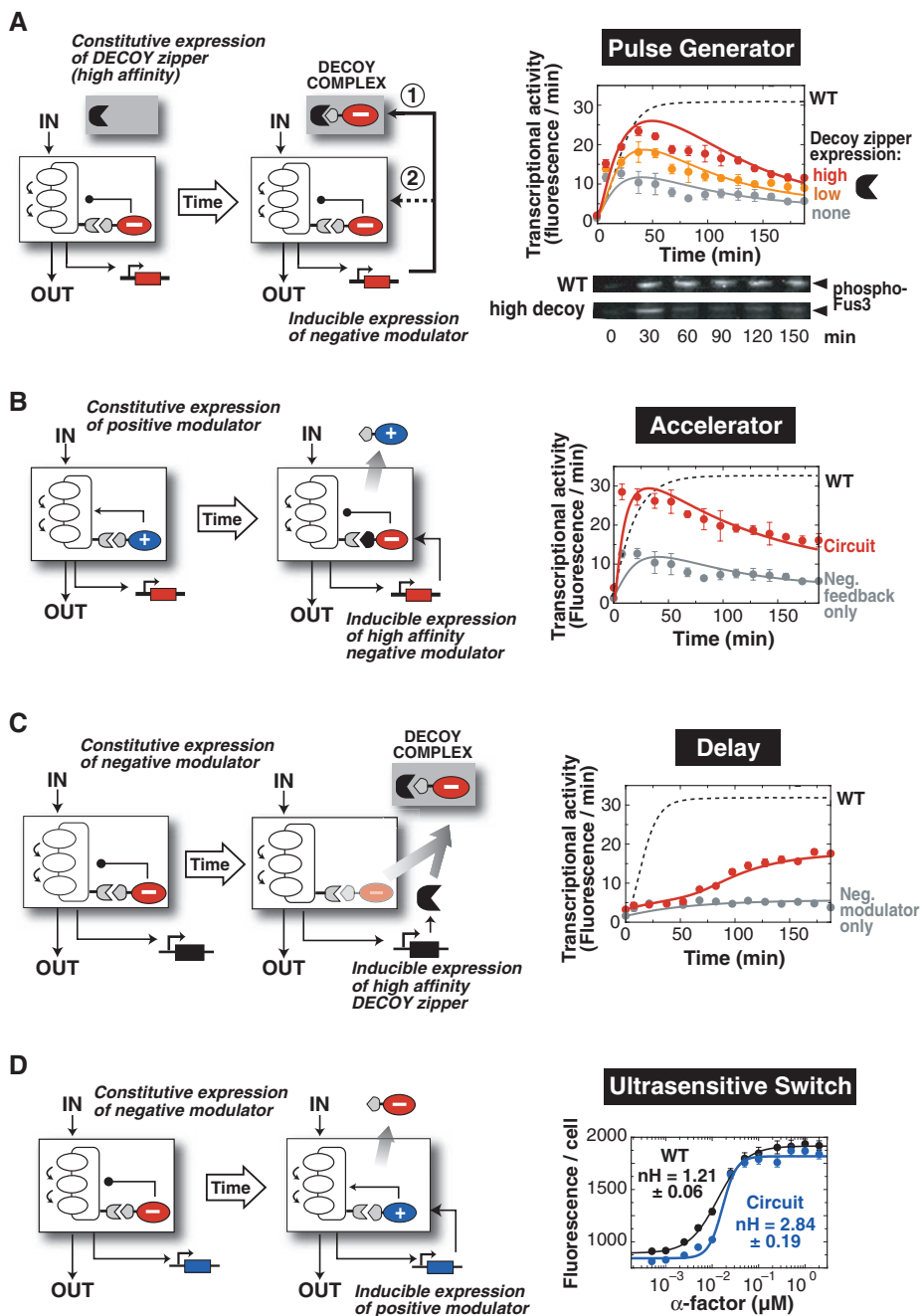


Fig. 4. Recruitment-based tool kit can be used to engineer diverse response behaviors. **(A)** Pulse behavior is built from simple negative-feedback loop (Fig. 2) by adding constitutively expressed decoy zipper (GST-zipper) that competes with the Ste5-zipper. Negative modulator (Msg5-zipper) is complementary to both Ste5 and decoy zippers, but decoy zipper binds with higher affinity ($K_d = 6.1$ versus 41 nM). When pathway is induced and negative modulator is expressed, decoy initially acts as binding sink. Only after decoy is saturated will modulator bind to scaffold and repress pathway flux. Circuit behavior monitored by *pFUS1*-GFP reporter (top) and antibody against phospho-Fus3 Western blot (bottom). **(B)** Accelerator circuit is generated by constitutively expressing positive modulator (promoter, *pSTE5*; gene, Ste50-zipper) combined with the simple negative-feedback loop (Fig. 2). Circuit reaches the maximal output observed for the wild-type circuit in <20 min (versus WT: ~ 75 min). **(C)** Delay response is generated by constitutively expressing negative modulator (promoter, *pSTE5*; gene, Msg5-zipper) and inducibly expressing decoy zipper that binds the negative effector-zipper (promoter, *pFIG1*; gene, GST-zipper) with higher affinity than the Ste5-zipper ($K_d = 6.1$ versus 41 nM). Negative modulator represses pathway until sufficient decoy zipper is expressed to relieve repression. **(D)** Enhanced ultrasensitive switch is built by constitutively expressing negative modulator (promoter, *pSTE5*; gene, Msg5-zipper) combined with the simple positive-feedback loop (Fig. 2). Negative modulator is displaced by inducibly expressed positive modulator (both have same zipper; $K_d = 41$ nM). Dose-response analysis shows increased ultrasensitivity (apparent Hill coefficient $n_H = 2.84 \pm 0.19$ versus WT, $n_H = 1.21 \pm 0.06$; simple positive-feedback loop, $n_H = 2.42$). See supporting online text for details on construction and analysis of these and related circuits.



behavior. We built a circuit with enhanced ultrasensitive switch behavior by constitutively expressing a negative modulator (Msg5-zipper) and inducibly expressing a positive modulator (Ste50-zipper) (Fig. 4D). This circuit is a double-positive-feedback loop—induced expression of Ste50-zipper directly increased pathway output, but also relieved the inhibitory effect of Msg5-zipper by displacing it from the scaffold. The dose-response profile for the resulting circuit showed an increase in cooperativity.

We have used a simple principle, recruitment of pathway modulators to a scaffold (32), to systematically alter a single MAPK pathway so that it displays a wide range of quantitative response behaviors. The evolutionary diversifi-

cation afforded by scaffolds may explain their common use in signaling pathways (33–37). The success of this simple recruitment-based engineering strategy suggests that it may be possible to reprogram cellular responses with high precision. In mammalian and plant cells, MAPK cascades play a central role in regulating differentiation, proliferation, apoptosis, immune response, and stress responses. Thus, the ability to tune MAPK signaling may facilitate the engineering of cells with novel therapeutic or biotechnological functions.

References and Notes

1. W. R. Burack, A. S. Shaw, *Curr. Opin. Cell Biol.* **12**, 211 (2000).
2. T. Pawson, J. D. Scott, *Science* **278**, 2075 (1997).

3. R. P. Bhattacharyya, A. Remenyi, B. J. Yeh, W. A. Lim, *Annu. Rev. Biochem.* **75**, 655 (2006).
4. B. N. Kholodenko, *Nat. Rev. Mol. Cell Biol.* **7**, 165 (2006).
5. J. W. Locasale, A. S. Shaw, A. K. Chakraborty, *Proc. Natl. Acad. Sci. U.S.A.* **104**, 13307 (2007).
6. J. E. Ferrell, *Sci. STKE* **2000**, PE1 (2000).
7. Materials and methods are available as supporting material on Science Online.
8. K. Y. Choi, B. Satterberg, D. M. Lyons, E. A. Elion, *Cell* **3**, 499 (1994).
9. J. A. Printen, G. F. Sprague, *Genetics* **138**, 609 (1994).
10. S. H. Park, A. Zarrinpar, W. A. Lim, *Science* **299**, 1061 (2003).
11. K. Harris *et al.*, *Curr. Biol.* **11**, 1815 (2001).
12. M. A. Poritz, S. Malmstrom, M. K. Kim, P. J. Rossmessl, A. Kamb, *Yeast* **18**, 1331 (2001).
13. A. Colman-Lerner *et al.*, *Nature* **437**, 699 (2005).
14. S. Paliwal *et al.*, *Nature* **446**, 46 (2007).
15. J. E. Ferrell Jr., E. M. Machleder, *Science* **280**, 895 (1998).

16. C. J. Marshall, *Cell* **80**, 179 (1995).
 17. S. Sasagawa, Y. Ozaki, K. Fujita, S. Kuroda, *Nat. Cell Biol.* **7**, 365 (2005).
 18. L. O. Murphy, J. Blenis, *Trends Biochem. Sci.* **31**, 268 (2006).
 19. M. Villedieu *et al.*, *Gynecol. Oncol.* **101**, 507 (2006).
 20. B. K. Choi, C. H. Choi, H. L. Oh, Y. K. Kim, *Neurotoxicity* **25**, 915 (2004).
 21. S. D. Santos, P. J. Verwee, P. I. Bastiaens, *Nat. Cell Biol.* **9**, 247 (2007).
 22. A. Acharya, S. B. Ruvinov, J. Gal, C. Vinson, *Biochemistry* **41**, 14122 (2002).
 23. M. Ramezani-Rad, *Curr. Genet.* **43**, 161 (2003).
 24. C. Wu, E. Leberer, D. Y. Thomas, M. Whiteway, *Mol. Biol. Cell* **10**, 2425 (1999).
 25. X. L. Zhan, R. J. Deschenes, K. L. Guan, *Genes Dev.* **11**, 1690 (1997).
 26. J. Andersson, D. M. Simpson, M. Qi, Y. Wang, E. A. Elion, *EMBO J.* **23**, 2564 (2004).
 27. R. P. Bhattacharyya *et al.*, *Science* **311**, 822 (2006).
 28. N. T. Ingolia, A. W. Murray, *Curr. Biol.* **17**, 668 (2007).
 29. N. Barkai, S. Leibler, *Nature* **387**, 913 (1997).
 30. B. Alberts *et al.*, *Essential Cell Biology* (Garland Science, London, ed. 2, 2003).
 31. N. Rosenfeld, M. B. Elowitz, U. Alon, *J. Mol. Biol.* **323**, 785 (2002).
 32. M. Ptashne, A. Gann, *Genes and Signals* (Cold Spring Harbor Laboratory Press, Cold Spring Harbor, NY, 2001).
 33. D. C. Popescu, A. J. Ham, B. H. Shieh, *J. Neurosci.* **26**, 8570 (2006).
 34. K. Scott, C. S. Zuker, *Nature* **395**, 805 (1998).
 35. F. D. Smith, L. K. Langeberg, J. D. Scott, *Trends Biochem. Sci.* **31**, 316 (2006).
 36. S. C. Strickfaden *et al.*, *Cell* **128**, 519 (2007).
 37. P. Mishra *et al.*, *Cell* **131**, 80 (2007).
 38. We thank H. El-Samad, T. Kortemme, H. Madhani, C. Tang, C. Voigt, J. Weissman, and the Lim laboratory for advice and comments. Supported by University of

California GREAT fellowship (C.J.B.), American Cancer Society Postdoctoral Fellowship (N.C.H.), Jane Coffin Childs Fellowship (S.Y.) and grants from the U.S. Defense Advanced Research Projects Agency (Biological Input/Output Systems); NIH Nanomedicine Development Centers (Roadmap); National Institute of General Medical Science, NIH; Packard Foundation; and Rogers Family Foundation (W.A.L.).

Supporting Online Material

www.sciencemag.org/cgi/content/full/319/5869/1539/DC1
 Materials and Methods
 SOM Text
 Figs. S1 to S6
 Tables S1 to S3
 References

1 October 2007; accepted 11 February 2008
 10.1126/science.1151153

Synaptic Theory of Working Memory

Gianluigi Mongillo,^{1*†} Omri Barak,^{2*} Misha Tsodyks^{2‡§}

It is usually assumed that enhanced spiking activity in the form of persistent reverberation for several seconds is the neural correlate of working memory. Here, we propose that working memory is sustained by calcium-mediated synaptic facilitation in the recurrent connections of neocortical networks. In this account, the presynaptic residual calcium is used as a buffer that is loaded, refreshed, and read out by spiking activity. Because of the long time constants of calcium kinetics, the refresh rate can be low, resulting in a mechanism that is metabolically efficient and robust. The duration and stability of working memory can be regulated by modulating the spontaneous activity in the network.

Working memory (WM) enables the temporary holding of information for processing purposes, playing a crucial role in the execution of a wide range of cognitive tasks (1). In the delayed-response paradigm, a stimulus that is briefly presented to an animal has to be kept for several seconds until the execution of a task. Enhanced, stimulus-specific spiking activity has been observed during this delay period and is considered to be a neuronal correlate of WM (2–5). The current theoretical framework holds that delay activity emerges either from intrinsic cell properties (6, 7) or as persistent reverberations in selective neural populations coding for different memories (8–12). These populations are formed during learning via long-term synaptic modifications (13). However, electrophysiological studies have shown that the delay activity increase can be very modest (14, 15), sometimes disappearing completely during part

of the delay period (16). These observations suggest that WM might not reside entirely in the spiking activity. Furthermore, holding information in a spiking form is energetically expensive because of the high metabolic cost of action potentials (17). Here, we present an alternative account based on properties of excitatory synaptic transmission in the prefrontal cortex (PFC) (18). The PFC is a cortical area implicated in WM (4), and excitatory synaptic transmission in this area can be markedly facilitatory, unlike sensory areas where it is mostly depressing (19, 20). We therefore propose that an item is maintained in the WM state by short-term synaptic facilitation mediated by increased residual calcium levels at the presynaptic terminals of the neurons that code for this item (21). Because removal of residual calcium from presynaptic terminals is a relatively slow process (22, 23), the memory can be transiently held for about 1 s without enhanced spiking activity.

We implemented this mechanism with a recurrent network of integrate-and-fire neurons (24). The network encodes a set of memories (items) by randomly composed selective populations of excitatory neurons (Fig. 1B). Connections between the neurons coding for the same memory are stronger than connections between different populations, mimicking the result of prior long-term Hebbian learning (25) or intrinsic clustering of recurrent connections (26). Inhibitory neurons are connected to the excitatory

ones in a nonstructured way, resulting in competition between different memories [see supporting online material (SOM)]. All excitatory-to-excitatory connections display facilitating transmission, described by a phenomenological model of short-term plasticity (20, 27). Synaptic efficacy is modulated by the amount of available resources (x , normalized so that $0 < x < 1$) and the utilization parameter (u) that defines the fraction of resources used by each spike, reflecting the residual calcium level (22, 23) (Fig. 1A and SOM). Upon a spike, an amount ux of the available resources is used to produce the postsynaptic current, thus reducing x . This process mimics neurotransmitter depletion. The spike also increases u , mimicking calcium influx into the presynaptic terminal and its effects on release probability. Between spikes, x and u recover to their baseline levels ($x = 1$ and $u = U$) with time constants τ_D (depressing) and τ_F (facilitating), respectively. The phenomenological model reproduces the behavior of cortical synapses, both depressing ($\tau_D > \tau_F$) and facilitating ($\tau_F > \tau_D$) (27). For PFC facilitating excitatory connections, the experimental fit reports $\tau_F \gg \tau_D$ (18), with τ_F on the order of 1 s.

The simulations begin with loading one item into WM by providing transient external excitation to the corresponding neural population (Fig. 2A). The population activity increases for the duration of the input, changing the internal state of the synaptic connections. The connections are both depressed (reduced x) and facilitated (increased u), with depression dominant on the time scale of τ_D and facilitation dominant on the time scale of τ_F (where $\tau_D = 0.2$ s and $\tau_F = 1.5$ s; see SOM for all parameter values). As long as the synapses remain facilitated, the memory can be reactivated by presenting a weak nonspecific excitatory input to the whole network (gray shading), even though the neural activity is at the spontaneous level. Reactivation is expressed as a short epoch of synchronized activity [“population spike” (PS)], where almost every neuron in the population fires a spike within an interval of about 20 ms (28, 29). Even though the reactivating signal is nonspecific (that is, it uniformly

¹Group for Neural Theory, Département d’Etudes Cognitives, Ecole Normale Supérieure et Collège-de-France, Paris, France.

²Department of Neurobiology, Weizmann Institute of Science, Rehovot, Israel.

*These authors contributed equally to this work.

†Present address: Laboratoire de Neurophysique et Physiologie, Université Paris-Descartes, CNRS-UMR8119, and Franco-Israeli Laboratory of System Neurophysiology and Neurophysics, Paris, France.

‡CNRS visiting member of the Group for Neural Theory, Ecole Normale Supérieure et Collège-de-France.

§To whom correspondence should be addressed. E-mail: misha@weizmann.ac.il